Supplemental Material

GLS1 governs vascular smooth muscle cell phenotypic switching and aortic dissection via glutamate metabolism

Authors

Wei Xie[1,#]; Chen Ning[3,#]; Chen Lu[1]; Dongjin Wang[4]; Shuang Zhao[3,*]; Tianyu Song[2,*]; Hailong Cao[1,*].

Affiliations

[1]Department of Cardiac Surgery, Zhongda Hospital, School of Medicine, Southeast University, Nanjing, Jiangsu, China;

[2]School of Medicine, Nanjing University of Chinese Medicine, Nanjing, Jiangsu, China;

[3]School of Pharmacy, Nanjing Medical University, Nanjing, Jiangsu, China.;

[4] Department of Cardiac Surgery, Nanjing Drum Tower Hospital, Affiliated Hospital of Medical School, Nanjing University, Nanjing, Jiangsu, China.

* Corresponding author

[#] These authors contributed equally

***Corresponding author:**

*Hailong Cao, MD, PhD.

Department of Cardiac Surgery, Zhongda Hospital, School of Medicine, Southeast University.

Address: No. 87 Dingjiaqiao, Gulou District, Nanjing, Jiangsu Province, 210009, China

Tel: +86-25-83262261

E-mail: hailongcao_zd@163.com; hailongcao@seu.edu.cn

*Tianyu Song, PhD.

School of Medicine, Nanjing University of Chinese Medicine.

Address: No. 138 Xianlin Avenue, Qixia District, Nanjing, Jiangsu Province, 210023, China

Tel: +86-15250966190

E-mail: tianyusong@njucm.edu.cn;

*Shuang Zhao, PhD.

School of Pharmacy, Nanjing Medical University.

Address: No. 101 Longmian Ave, Jiangning District, Nanjing, Jiangsu, 211166, China

Tel: +86-15720800551

E-mail: zhaoshuang@njmu.edu.cn.

Supplemental Tables

Supplemental table S1. The characteristics of patients

Patients	Age (years)	Gender	Smoking	BMI (kg/m^2)	Hypertension	Diabetes mellitus	Hyperlipidemia
Non-AD1	58	Male	No	23.1	Yes	No	No
Non-AD2	67	Female	Yes	26.7	No	No	Yes
Non-AD3	54	Female	No	22.9	Yes	Yes	Yes
Non-AD4	62	Male	Yes	25.3	No	No	No
Non-AD5	63	Female	No	24.5	No	No	No
AD1	59	Male	No	24.8	Yes	No	Yes
AD2	68	Female	Yes	27.2	No	No	No
AD3	55	Male	No	23.6	Yes	No	No
AD4	72	Female	Yes	25.9	Yes	Yes	No
AD5	60	Female	No	26.0	Yes	No	Yes
AD6	64	Male	No	24.2	Yes	No	No
AD7	57	Female	Yes	25.5	No	No	No
AD8	63	Male	No	23.8	Yes	No	No

Variables	Non-AD (n=5)	AD(n=8)	*P* value
Age (years, Mean ± SD)	60.8 ± 5.0	62.3 ± 5.7	0.65
Male (N, %)	2 (40%)	4 (50%)	1.00
Smoking (N, %)	2 (40%)	3 (37.5%)	1.00
BMI (kg/m^2, Mean ± SD)	24.5 ± 1.6	25.1 ± 1.2	0.44
Hypertension (N, %)	2 (40%)	6 (75%)	0.29
Diabetes mellitus (N, %)	1 20%)	1 (12.5%)	1.00
Hyperlipidemia (N, %)	2 (40%)	2 (25%)	1.00

Supplemental table S2. The characteristics of GEO datasets

GEO accession	Platform	Organism	Samples
GSE52093	GPL10558	Homo sapiens	5 normal human aortas and 7 aortas from AD patients
GSE98770	GPL14550	Homo sapiens	5 transplant donor aortas and 6 aortas from AD patients
GSE213740	GPL18573	Homo sapiens	3 normal human aortas and 6 aortas from AD patients

Supplemental table S3. Primary and secondary antibodies used in this study

Target	Host pecies	Supplier	Catalog No.
GLS1	Rabbit polyclonal	Proteintech	12855-1-AP
RARα	Rabbit monoclonal	Abcam	ab275745
TAGLN	Mouse monoclonal	Abcam	ab14106
ACTA2	Rabbit monoclonal	Abcam	ab124964
OPN	Rabbit polyclonal	Abcam	ab8848
ACTA2	Mouse monoclonal	Santa Cruz Biotechnolog	sc-53015
GAPDH	Mouse monoclonal	Abways Technology	AB0037
β-Actin	Mouse monoclonal	Abways Technology	AB0035
FLAG tag	Mouse monoclonal	Proteintech	66008-3-Ig
PI3K	Rabbit monoclonal	Cell Signaling Technology	4257T
AKT	Rabbit monoclonal	Cell Signaling Technology	4691T
mTOR	Rabbit monoclonal	Cell Signaling Technology	2983T
Phospho-AKT (Ser473)	Rabbit monoclonal	Cell Signaling Technology	4060T
Phospho-mTOR (Ser2448)	Rabbit monoclonal	Cell Signaling Technology	5536T
Phospho-PI3K	Rabbit monoclonal	Affinity Biosciences	AF-3241
Alexa Fluor® 594 anti-mouse IgG	Donkey polyclonal	Thermo Fisher Scientific	A21203
Alexa Fluor® 594 anti-rabbit IgG	Donkey polyclonal	Thermo Fisher Scientific	A21207
Alexa Fluor® 488 anti-mouse IgG	Donkey polyclonal	Thermo Fisher Scientific	A21202
Alexa Fluor® 488 anti-rabbit IgG	Donkey polyclonal	Thermo Fisher Scientific	A21206
HRP-conjugated anti-mouse IgG	Goat polyclonal	Thermo Fisher Scientific	31430
HRP-conjugated anti-rabbit IgG	Goat polyclonal	Thermo Fisher Scientific	31460

Supplemental table S4. The primer sequences used for qRT-PCR analysis

Gene	Forward (5' to 3' sequence)	Reverse (5' to 3' sequence)	Species
GLS1	TCTACAGGATTGCGAACGTCT	CTTTGTCTAGCATGACACCATCT	Human
RARα	GGGCAAATACACTACGAACAACA	CTCCACAGTCTTAATGATGCACT	Human
GAPDH	GGAGCGAGATCCCTCCAAAAT	GGCTGTTGTCATACTTCTCATGG	Human
ACTA2	AAAGCAAGTCCTCCAGCGTT	TAGTCCCGGGGATAGGCAAA	Human
TAGLN	GGAAACCCACCCTCTCAGTC	TGCACTAGCCAAGTCATCCG	Human
OPN	ATCTCCTAGCCCCACAGACC	CACACTATCACCTCGGCCAT	Human
Gls1	GATGGCCCTAGGATGTCTGC	GCTGACTTGCCCACTCTCAT	Mouse
Rarα	TTCTTTCCCCCTATGCTGGGT	GGGAGGGCTGGGTACTATCTC	Mouse
18S	AGTCCCTGCCCTTTGTACACA	CGATCCGAGGGCCTCACTA	Mouse
Opn	AATCTCCTTGCGCCACAGAA	GGACATCGACTGTAGGGACG	Mouse
Acta2	CGCCTCCAGTTCCTTTCCAA	AGAGGGGGCCACCCTATAAT	Mouse
Tagln	AGGGGTGACATCACTGCCTA	GACTGCACTTCTCGGCTCAT	Mouse

Supplemental Figures and Figure Legends

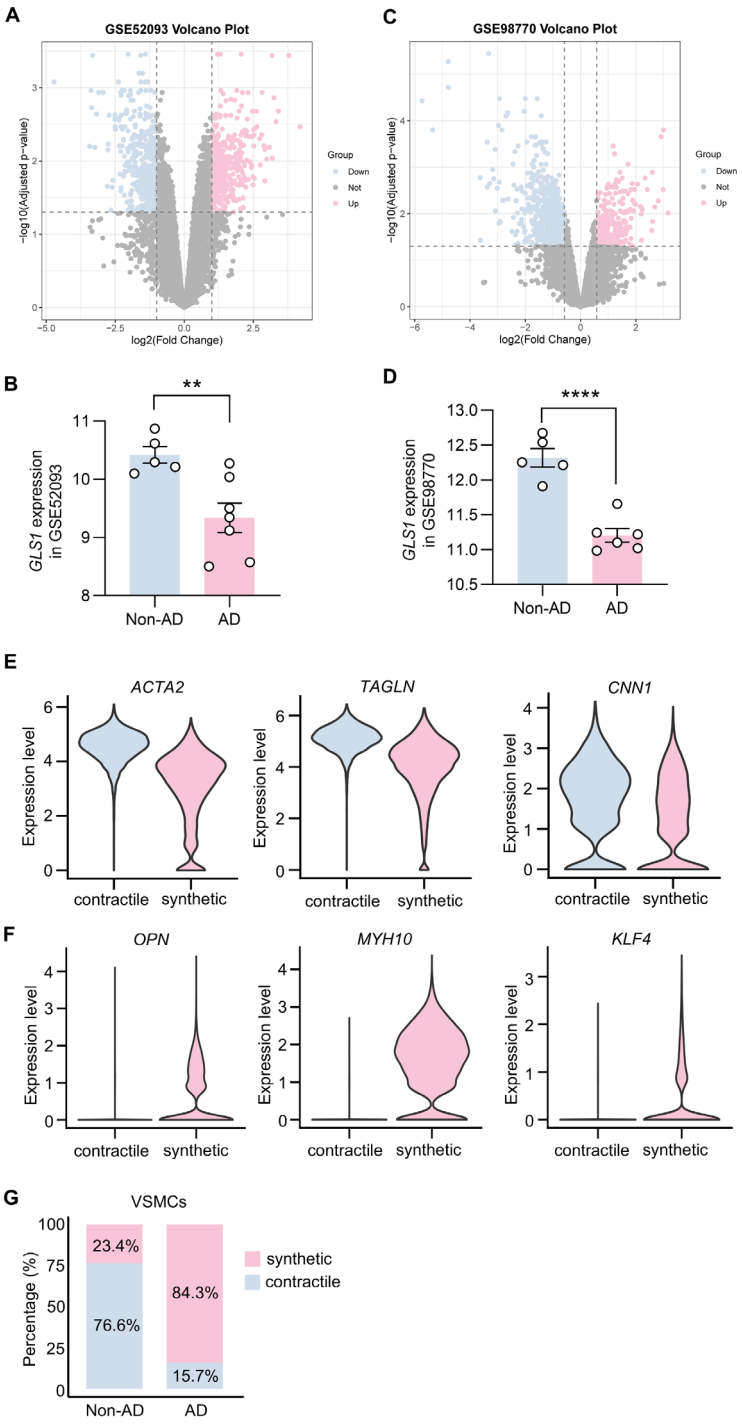

Supplemental Figure S1. GLS1 expression is reduced in aortic dissection.
(A) Volcano plot illustrating differentially expressed genes in human aortic dissection database (GSE52093), with upregulated (red) and downregulated (blue) genes indicated. **(B)** The relative *GLS1* expression in the aorta of Non-AD and AD patients according to GSE52093. **(C)** Volcano plot illustrating differentially expressed genes in human aortic

dissection database (GSE98770), with upregulated (red) and downregulated (blue) genes indicated. **(D)** The relative *GLS1* expression in the aorta of Non-AD and AD patients according to GSE98770. **(E)** The expression of contractile markers (ACTA2, TAGLN, CNN1) in synthetic VSMCs (cluster_2) and contractile VSMCs (cluster_5). **(F)** The expression of synthetic markers (OPN, MYH10, KLF4) in synthetic VSMCs (cluster_2) and contractile VSMCs (cluster_5). **(G)** The proportion of contractile and synthetic VSMCs in Non-AD and AD groups. Data are presented as mean ± SEM. Statistical analysis was performed using unpaired, two-tailed Student's *t* test (**C** and **D**). $^{**}p < 0.01$, $^{****}p < 0.0001$.

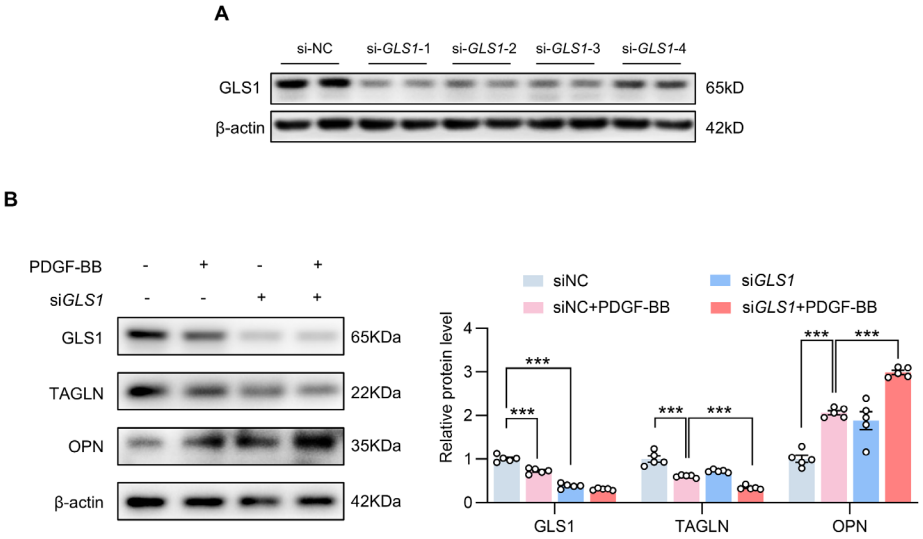

Supplemental Figure S2. *GLS1* knockdown aggravates VSMCs phenotypic switching.

(A) The efficiency of si*GLS1* in HASMCs was detected by Western blot. **(B)** HASMCs were transfected with siRNA against *GLS1* (si*GLS1*) or negative control (siNC), and then treated with PDGF-BB. Western blot and quantitative analysis of GLS1, TAGLN and OPN expression in HASMCs. Data are presented as mean ± SEM. Statistical analysis was performed using one-way ANOVA followed by Tukey's multiple-comparison test (**B**). ***$p < 0.001$.

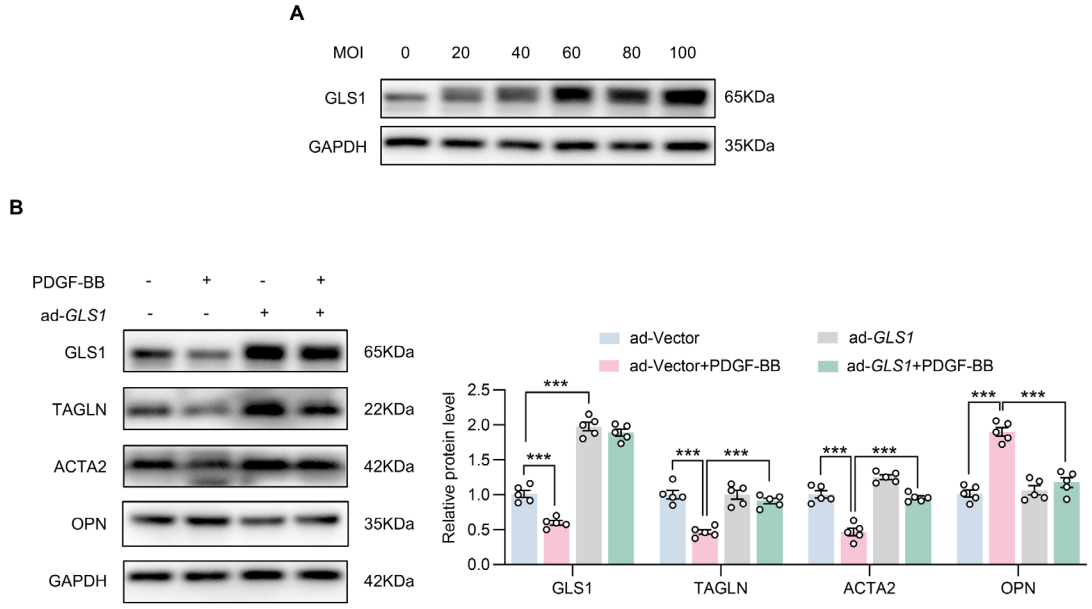

Supplemental Figure S3. GLS1 overexpression alleviates VSMCs phenotypic switching.

(A) The efficiency of different concentration of adenovirus mediated GLS1 overexpression in HASMCs was detected by Western blot. **(B)** HASMCs were infected with adenovirus containing empty vector (ad-Vector) or GLS1-encoding plasmids (ad-*GLS1*), and then treated with PDGF-BB. Western blot and quantitative analysis of GLS1, TAGLN, ACTA2 and OPN expression in HASMCs. Data are presented as mean ± SEM. Statistical analysis was performed using one-way ANOVA followed by Tukey's multiple-comparison test (**B**). ***p < 0.001.

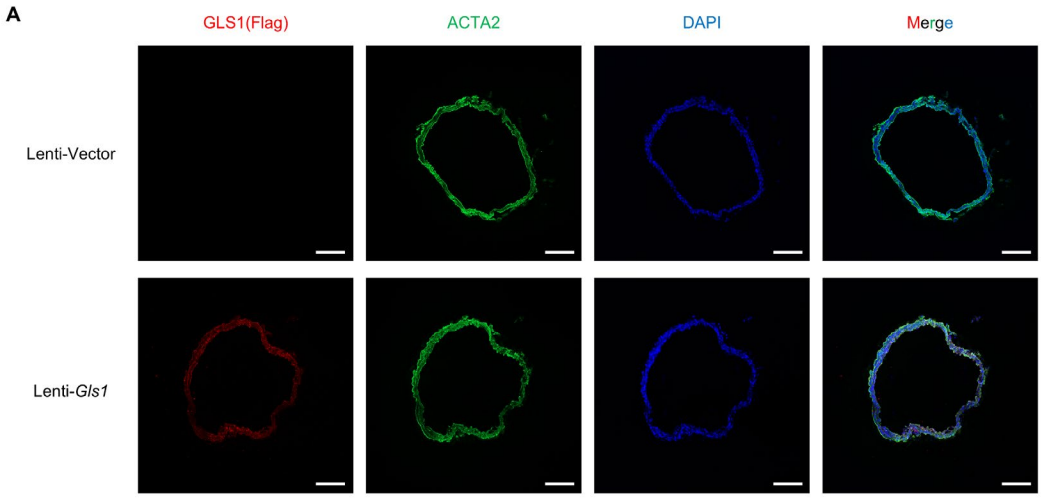

Supplemental Figure S4. The efficiency of exogenous GLS1 expression in VSMCs of aorta.

(A) Three-week-old male *Tagln*$^{Cre/+}$ mice were intravenously injected with lentivirus containing control vector or reverse *Gls1* sequence with two *loxP* sites. The expression of exogenous GLS1 was detected by immunofluorescence staining for Flag (red), ACTA2 (green) and DAPI (blue) in mice aorta sections. Scale bars, 200 μm. n = 3.

A

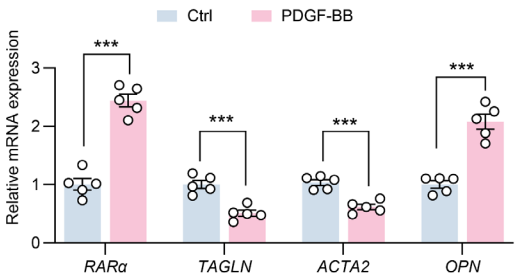

Supplemental Figure S5. RARα expression is increased in PDGF-BB treated HASMCs.

(A) HASMCs were treated with PDGF-BB. The mRNA expression of *RARα*, *TAGLN*, *ACTA2* and *OPN* in HASMCs was detected by qRT-PCR. Data are presented as mean ± SEM. Statistical analysis was performed using unpaired, two-tailed Student's *t* test (**A**). ***$p < 0.001$.

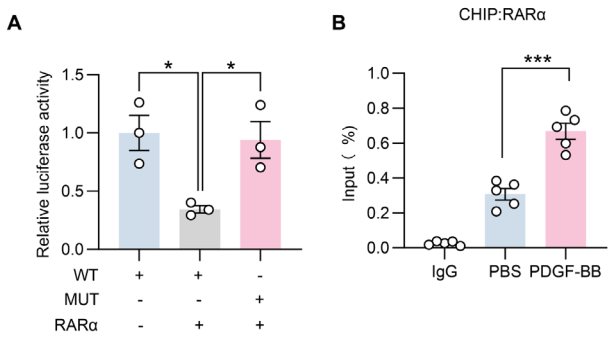

104

105 **Supplemental Figure S6. Verification of the binding of RAR to *GLS1* promoter.**
106 **(A)** Relative luciferase activity in HASMCs co-infected with adenoviruses carrying
107 either the wild-type *GLS1* promoter or its transcription factor binding site 2 (TFBS2)
108 mutant luciferase reporter constructs, along with adenovirus expressing RARα. **(B)**
109 HASMCs were treated with PDGF-BB. Chromatin immunoprecipitation (ChIP) assays
110 were performed with IgG or anti- RARα antibody, followed by qRT-PCR with primers
111 targeting *GLS1* promoter regions. Data are presented as mean ± SEM. Statistical
112 analysis was performed using one-way ANOVA followed by Tukey's multiple-
113 comparison test (**A**) and unpaired, 2-tailed Student's *t* test (**B**). *$p < 0.05$, ***$p < 0.001$.
114

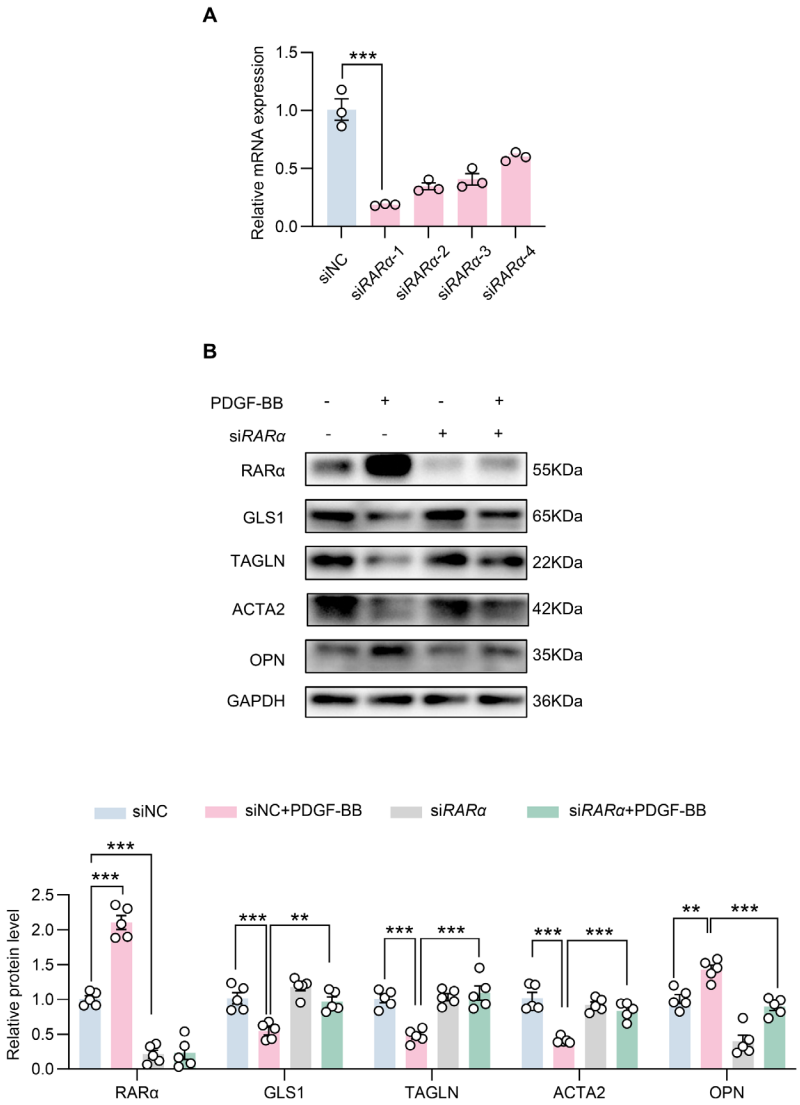

Supplemental Figure S7. *RARα* knockdown alleviates VSMCs phenotypic switching.

(A) The efficiency of si*RARα* in HASMCs was detected by qRT-PCR. **(B)** HASMCs were transfected with siRNA against *RARα* (si*RARα*) or negative control (siNC), and then treated with PDGF-BB. Western blot analysis of RARα, GLS1, TAGLN, ACTA2 and OPN expression in HASMCs. Data are presented as mean ± SEM. Statistical analysis was performed using one-way ANOVA followed by Tukey's multiple-comparison test (**C**). **p < 0.01, ***p < 0.001.